



Effect of Mn and Zr Addition on Microstructure, Wear and Corrosion Behavior of Ti-6Al-4V Composite Biomaterials Produced by Powder Metallurgy

Harun Çuğ^{1,*} , Mohamed E. E. Erhaima² 

¹Karabük University, Engineering Faculty, Karabük, Turkey

²Karabük University, Graduate Education Institute, Karabük, Turkey

ARTICLE

INFORMATION

Received: 09.08.2021

Accepted: 26.08.2021

Keywords:

Ti-6Al-4V

Composite

Wear

Corrosion

ABSTRACT

In this study, composite biomaterials were produced by powder metallurgy (P/M) method. Ti-6Al-4V master alloy and different proportions of Mn and Zn have been added to this alloy. Dry wear test and electrochemical corrosion test in Hank fluid (Body fluid) were applied to the produced composite P/M materials. The addition of Mn in the produced materials was effective in improving the wear behavior of the Ti-6Al-4V composite material. In addition, the addition of Zr provided excellent corrosion resistance in Hank's solution. The superior properties of Ti-6Al-4V composite material with its microalloy approach are quite challenging for biomedical applications. The best wear resistance was achieved by adding 2%Mn to Ti-6Al-4V by weight. In addition, it was observed that the phases formed as a result of the addition of 2% Zr act as a barrier during corrosion.

Toz Metalurjisi ile Üretilen Ti-6Al-4V Kompozit Biyomalzemelerin Mikroyapı, Aşınma ve Korozyon Davranışlarına Mn ve Zr İlavesinin Etkisi

MAKALE BİLGİSİ

Alınma: 09.08.2021

Kabul: 26.08.2021

Anahtar Kelimeler:

Ti-6Al-4V

Kompozit

Aşınma

Korozyon

ÖZET

Bu çalışmada toz metalurjisi yöntemi kompozit biyomalzeme üretimi yapılmıştır. Ti-6Al-4V master alaşımı ve bu alaşıma farklı oranlarda Mn ve Zn ilave edilmiştir. Üretilen kompozit malzemelere kuru aşınma deneyi ve Hank sıvısı (Vücut sıvısı) içerisinde korozyon testi uygulanmıştır. Üretilen malzemelerde Mn ilavesi Ti-6Al-4V kompozit malzemenin aşınma davranışını iyileştirmede etkili olmuştur. Ayrıca Zr ilavesi Hank çözeltisinde 37°C'de mükemmel korozyon direnci sağlamıştır. Mikroalaşım yaklaşımı ile Ti-6Al-4V kompozit malzemenin üstün özellikleri, biyomedikal uygulamalar için oldukça iddialıdır. En iyi aşınma direnci ağırlıkça %2Mn Ti-6Al-4V ilavesiyle oluşturulmuştur. Ayrıca %2Zr ilavesi sonucu oluşan fazların korozyon esnasında bariyer olarak görev yaptığı görülmüştür.

1. INTRODUCTION

Titanium (Ti) composite materials have achieved admirable recognition in the last couple of decades by engineering applications such as biomedical and vehicle parts because of their superior corrosion resistance and outstanding mechanical properties in different environmental conditions [1]. The production of Ti composite materials are encountering some problems as regard manufacturing cost that resulted from their high melting point during casting, multiple processes along with shaping and design hindrance [2]. Powder metallurgy (PM) is the alternative production method to solve mentioned problems and makes economically complex-shaped parts simply for engineering applications [3]. To improve the mechanical properties of Ti composite materials Zr has been added to β -type Ti composite materials which present close young modulus values of human bone thus limiting the stress shielding effect during service time [4]. As to Ti-6Al-4V, it is the most used Ti composite materials for especially biomedical parts, the improving the corrosion resistance of Ti-6Al-4V was studied by elements such as Si [5], V [6], Mo [7] and Nb [8]. The

* Corresponding author, e-mail: hcug@karabuk.edu.tr

<https://doi.org/10.52795/mateca.980472>

controlling of corrosion attacks by composite material elements could be accomplished by the composition amount, phase types and changing of microstructure [9]. Moreover, stable oxide particles make an important role to diminish the rate of corrosion as the passive layer occurs on the surface [10]. Many studies have been reported about the effect of the Zr on the corrosion resistance of Ti base composite materials [11-13]. However, the little report was published about Ti-6Al-4V composite materials among these literatures [14, 15]. As for Mn, it is stable on the microstructure that is suppressing the β -type phase thanks to the solid solution hardening effect [16]. Moreover, it is an essential element for human life to continue during daily life. Furthermore, it has similar effects with base Ti because cell viability is exceptional when the amount in the composition below 13% [17]. In this study, the Ti-6Al-4V materials produced by the PM method where the both Mn and Zr amount are determined with 0.5, 1 and 2 in wt% to be added. The electrochemical behavior of Ti-6Al-4V, Ti-6Al-4V-xMn and Ti-6Al-4V-xZr was investigated in Hank's solution at 37 °C. The dry wear test of produced composite materials was accomplished at 25°C. To observe the microstructure, scanning electron microscopy (SEM) was utilized that supported by energy dispersion spectrometer (EDS).

2. MATERIAL AND METHOD

Ti-6Al-4V-xMn and Ti-6Al-4V-xZr composite materials (x=0, 0.5, 1 and 2 wt%) were produced by powder metallurgy method, where titanium powder (99.7%, d <149 μ m, Nanografi), aluminum (91%, d <50 μ m, Nanografi), vanadium (99.5%, d <44 μ m, Nanografi), manganese (99.5%, d <44 μ m, Nanografi) and zirconia (99.5%, d <44 μ m, Nanografi) for Ti6Al4V alloy powders were used. The produced composite materials labeled as base, 0.5Mn, 1Mn, 2Mn, 0.5Zr, 1Zr, 2Zr for Ti-6Al-4V, Ti-6Al-4V-0,5Mn, Ti-6Al-4V-1Mn, Ti-6Al-4V-2Mn, Ti-6Al-4V-0,5Zr, Ti-6Al-4V-1Zr and Ti-6Al-4V-2Zr, respectively. Powder metallurgy was used to manufacture the investigated composite materials. Mixing was carried out on a rocking mill machine for 60 minutes; In addition, 0.15 g of the lubricant oil was applied to evenly distribute the supplements in the Ti powder. The sintering temperature is applied at 800 C. The compact was sintered at 800 C for 1.8 ks at a pressure of 20 MPa under a vacuum of 4 Pa. The resulting sintered billet has a diameter of 8 mm and a height of 12 mm. These conditions were the same for all sample preparation.

The microstructure of investigated composite materials were characterized by scanning electron microscopy (SEM, Zeiss Ultra Plus Gemini Fesem) where, metallographic techniques such as grinding and polishing were applied with the end of mirror surface after that etching is performed by Kroll's reagent (80H₂O, 15 ml of HNO₃ and 5 ml of HF).

Electrochemical corrosion testing was performed for the Ti-6Al-4V-xMn and Ti-6Al-4V-xZr composite materials (8mmx8mm) at temperature of 36.5°C. Potentiodynamic tests were performed with parstat 4000 potentiostat machine which based on the three electrode setup, where specimens, Ag / AgCl (3.5 mol KCl) and a pair of graphite rods are the working electrode, reference electrode and counter electrode, respectively. The sample preparation was accomplished by following procedure. Firstly, the samples were grinding by 2500 grit SiC and polished with diamond suspension of 3 μ m. Secondly, the surface cleaning was finished by ultrasonic cleaning in acetone and deionized water. The test duration is determined as 900s at a scan rate of 2 mV / s in a scanning interval of -0.75 V vs. Ag/AgCl to +0.50 V vs. Ag/AgCl. Hank's solution [18] is applied as a corrosive environment.

Wear tests carried out at 25°C. 8 mm bulk materials were exposed to wear along 40 m under load 60 N (6kg) with 0,5mm/s wear speed at 25 °C according to ASTM-G133 which was conducted in a tribometer. The counterbody component was steel AISI 52100 (analog ShKh15) with a hardness of 61 HRC. Before the wear test, the sample surfaces were first sanded with 1200 grit and dried with alcohol before the wear test. After the wear test, microstructure images of the samples were taken by digital microscope (Nikon SHUTTLEPIX Digital Microscope) and SEM (Carl Zeiss Ultra Plus Gemini Fesem). The wear volume of each specimen was found by multiplying the stroke distance and the cross-sectional area under 2D curves in the transverse direction of the wear track. The 2D area was measured with a Mitutoyo SJ-410 instrument using a standard probe with a diameter of 2

mm at five different locations depending on the depth (h) and width (L) of the wear scar. 2D area measurements were made according to the ISO 4287 standard. Hardness of samples was measured by micro-vickers (HV1) of load 10 N.

3. RESULTS AND DISCUSSION

3.1. Microstructure

The phases were determined with α and β phases for both investigated Mn and Zr added composite materials which are given in Fig.1 [3]. As to all investigated composite materials, the dark region is obtained as β phase, however, the light appears as α phase. It is shown that base labelled composite material contains the fine acicular α -phases and broader β -phase is around by lath- α phase. As to adding of Mn to Ti-6Al-4V, the amount of 0.5 wt% Mn enhanced the formation of a broader α -phase that encircled the equiaxed β -phase. As for the Mn, addition is 1 wt%, the microstructure is reverted to the initial micrograph of Ti-6Al-4V which has the fine α -phase placed on the boundaries of β -phase. Regarding the 2 wt% Mn addition, the β -phase formed clearly which is surrounded by lath- α phase. On the other hand, the β -phase became more dominant than α -phase on the microstructure of 0.5Zr labelled composite material where the formed acicular α -phase has outstretched arms along β -phase. The β -phase was replaced by intergranular β -phase with the addition of 1wt% Zr, however, the α -phase is similar with 0,5wt% Zr added one. 2Zr labelled composite material contains laves phase [19] that occurred as lighter white and morphologically platelet which mostly was placed along the boundaries of β -phase and partially inside of the lath α -phase.

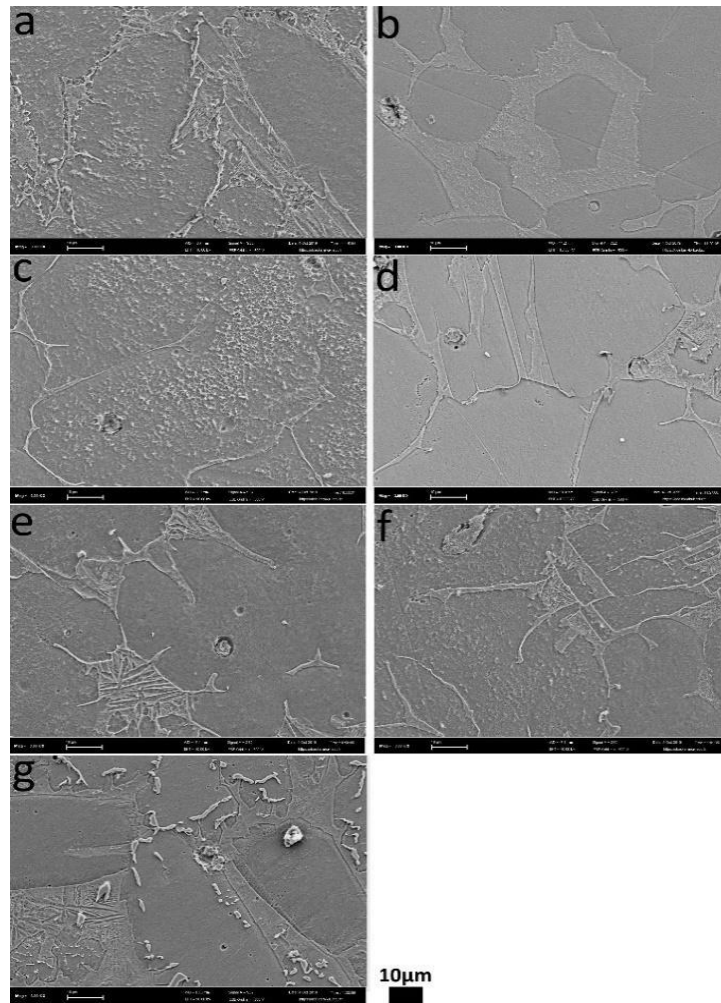


Figure 1. SEM micrographs of (a) base, (b) 0.5Mn, (c) 1Mn, (d) 2Mn, (e) 0.5Zr, (f) 1Zr and (g) 2Zr composite materials ((a) baz, (b) 0.5Mn, (c) 1Mn, (d) 2Mn, (e) 0.5Zr, (f) 1Zr ve (g) 2Zr kompozit malzemelerin SEM mikrografları)

3.2. Corrosion test

The potentiodynamic polarization curves enable to investigate the effect of Mn and Zr addition to the corrosion resistance of Ti-6Al-4V composite materials in the simulated body fluid environment. The potentiodynamic polarization curves for investigated composite materials that base, Mn and Zr added composite materials were illustrated in Fig.2 and the test results were given in Table 1. As seen in Fig. 2, the noticeable transition region is not obtained from active and passive curves. On the other hand, when we look at the Fig.3, the corrosion current density (CCD) of 2Zr labelled composite materials has the lowest value of $0.004 \mu\text{A} / \text{cm}^2$ that followed by 2Mn and base labelled composite materials that values of 0.350 and $0.526 \mu\text{A} / \text{cm}^2$, respectively. However, the highest ones as CCD were presented by 0.5Zr and 1Zr composite materials with the values of 1.173 and $1.480 \mu\text{A} / \text{cm}^2$, respectively. As to the corrosion rate values that are proportional to the CCD, as seen in Table 1. The different behaviour of corrosion resistance of investigated composite materials could have resulted from the changing of microstructure that showed distinctive phases formed based on the amount of %wt Mn and Zr. The role of the occurred phases here could be explained by the role of corrosion barrier where the homogeneously distributed phases impart to more resistance regions to corrosive attacks due to anodic and cathodic behaviour of materials was changed by these regions [20]. The addition of 0.5 %wt Mn to base changed the α phase as broader and therefore worse corrosion resistance was obtained than the base. The finer α phase gives rise to better corrosion resistance that is approved by 1Mn composite material containing both microstructure and CCD values closely with base composite material. The different corrosion behaviour of base and 1Mn labelled composite materials could have resulted from the lath α phase forming a higher amount inside base one. Similarly, the lath α phase is enclosed the β -phase homogeneously. On the other hand, a minor amount of Zr addition to base composite material makes microstructure different where a particular α phase has the arms spread to β -phase. It is clear that from the microstructure image of the 1Zr composite material, acicular α phase was more formed inhomogeneously than 0.5Zr that worsened the corrosion rate. However, the Laves α phase obtained from the addition of 2Zr%wt impart to best corrosion resistance because of their distribution of grain boundaries homogeneously that give rise to a better barrier to corrosion attacks.

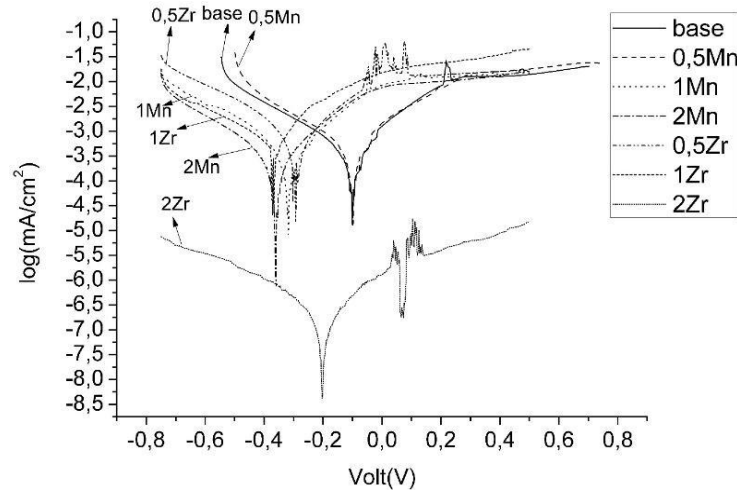


Figure 2. The potentiodynamic polarization curves of tested composite materials in Hank's solution (Hank'in çözümünde test edilen kompozit malzemelerin potansiyodinamik polarizasyon eğrileri)

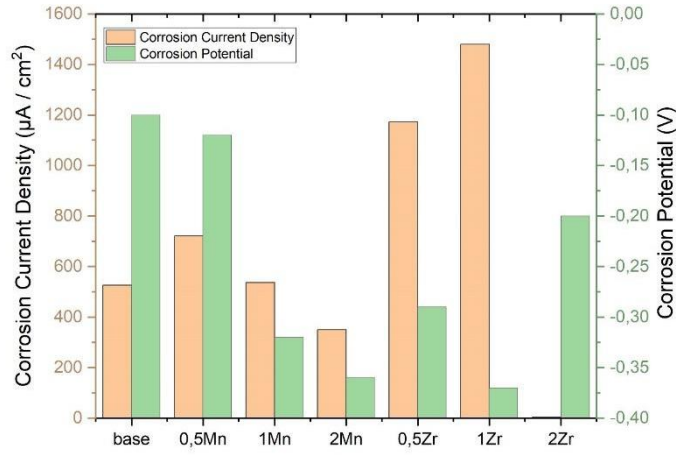


Figure 3. Variation of experimental corrosion potential and corrosion current density with Mn and Zr contents of Ti-6Al-4V composite materials (Ti-6Al-4V kompozit malzemelerin Mn ve Zr içerikleri ile deneysel korozyon potansiyeli ve korozyon akım yoğunluğunun değişimi)

Table 1. The potentiodynamic corrosion test results (Potansiyodinamik korozyon testi sonuçları)

Materials	S.A (cm ²)	d (g / cm ³)	E.W	CC (µA)	CCD (µA / cm ²)	CR (mm / year)	E _{corr} (V)
Base	0.283	4.22	23.10	0.149	0.526	0.009	-0.10
0.5Mn	0.283	4.30	23.25	0.204	0.721	0.013	-0.12
1Mn	0.283	4.17	23.35	0.152	0.537	0.010	-0.32
2Mn	0.283	4.27	23.60	0.099	0.350	0.006	-0.36
0.5Zr	0.283	4.31	23.25	0.332	1.173	0.021	-0.29
1Zr	0.283	4.28	23.35	0.419	1.480	0.026	-0.37
2Zr	0.283	4.30	23.60	0.001	0.004	8x10 ⁻⁶	-0.20

Labels: CC: Corrosion Current, CCD: Corrosion Current Density, CR: Corrosion Rate, E_{corr} : Corrosion Potential, d: density, S.A: Surface Area, E.W: Equivalent Weight

3.3. Hardness Test

The hardness test results of the investigated composite materials are presented in Fig. 4. As seen from Fig.4, the highest and the lowest values were obtained from 0.5Zr (359HV) and 2Zr (419HV) labelled composite materials, respectively. When we investigate the effect of the amount Mn to hardness, there is an increase with the addition of 0.5 wt. % Mn (383HV) which is similar to almost 1 wt. % Mn (380HV) added one due to the enlarged α -phase and β -phase. Further, the hardness is increasing with the addition of the 2 wt. % Mn (417HV) to base composite material (376HV) as the lath α -phase. It is known that the grain boundaries impart more hindering to dislocation movement which is attributing to the rising of hardness. However, the smooth character of α and β phase gives rise to lower hardness to Ti composite materials. As we look at the microstructure of the Zr added composite materials, it draws a parallel between the broader continuously formed β -phase and hardness increasing as the β phase is enlarged on the microstructure where, the hardness measurement was obtained as 359HV, 374HV and 419HV for 0.5Zr, 1Zr and 2Zr labelled composite materials, respectively. The highest hardness inside Zr added composite materials was measured at 2Zr labelled composite material contains Laves phase distribution especially on grain boundaries of β phase where the increasing hardness could be resulted from the extra boundaries to resist the dislocation movements [11].

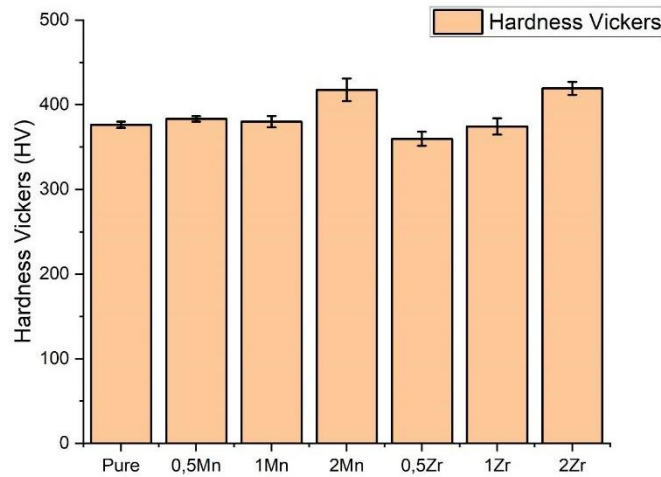


Figure 4. The micro vickers hardness test results of investigated composite materials (İncelenen kompozit malzemelerin mikro vickers sertlik testi sonuçları)

3.4. Wear Test

The wear volume of the investigated composite materials was illustrated in Fig.5-6. Moreover, the SEM images are providing the plastic deformation and oxidation type wear mechanisms that occurred during the wear test for all specimens. The morphology of wear tracks belonging to all specimens is obviously similar that indicates the wear mechanism mostly was imparted by the adhesive wear process. To understand the relationship wear volume loss of investigated composite materials between microstructures, the EDS study was utilized. The results obtained by EDX analysis showed that the oxide formation with the addition of Mn and Zr particles changed the wear volume proportionally with the MnO or ZrO₂. As to Mn addition between 0.5wt% and 2%wt, the MnO formation is firstly is increased but after that, it is decreasing and lastly again increasing that was observed for 0.5%wt Mn, 1%wt Mn and 2%wt Mn addition, respectively. In addition, the ZrO₂ formation showed similar behavior with the addition of %wt Zr addition, where the amount of ZrO₂ is as 2Zr>1Zr>0.5Zr. It could be said that the stable oxide particle resists the high contact pressure during wear test. To compare the wear volume of investigated composite materials, it can be said the wear resistance of base composite material was improved by the addition of the Mn and Zr particles. The lowest wear volume loss is obtained at 2Mn and 2Zr composite materials which have almost close values however, 2Zr is lower than 2Mn. In addition, the hardness result confirms the wear resistance of composite materials as the harder material the more resistant to counter material.

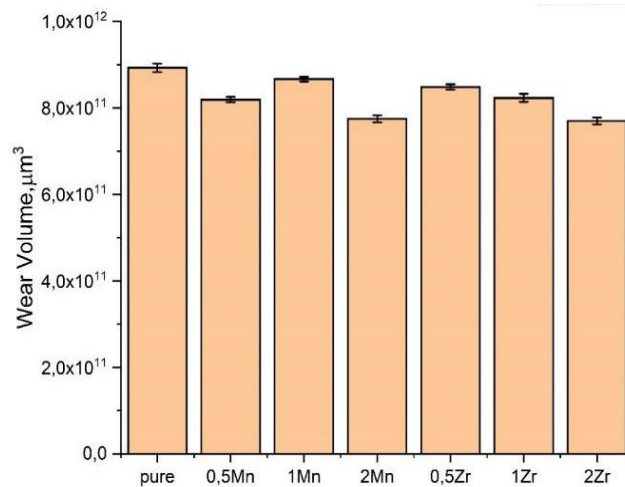


Figure 5. The wear volume of investigated composite materials (İncelenen kompozit malzemelerin aşınma hacmi)

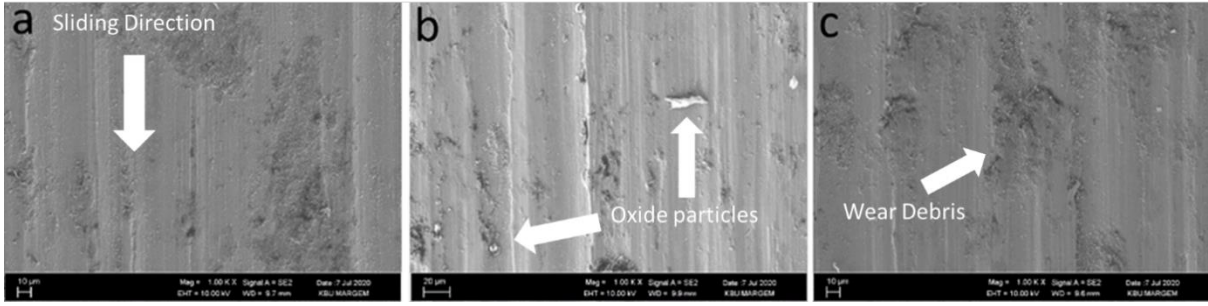


Figure 6. The worn surface of (a) base, (b) 2Mn and (c) 2Zr labelled composite materials ((a)Baz, (b) 2Mn ve (c) 2Zr etiketli kompozit malzemelerin aşınmış yüzeyi)

The worn surfaces of the base, 2Mn and 2Zr labelled composite materials are given in Fig. 6. It can be seen that wear scratches are parallel to sliding direction (Fig. 6a). This indicates that abrasive wear mechanism is formed [21]. Also, there are oxide particles on wear surfaces (Fig. 6b). Therefore, it shows that oxidation type wear mechanism formed on the wear surfaces of composite materials. Besides, abrasive wear marks, micro grooving and fractures are seen in some regions. Thus, it can be noted that abrasive wear mechanism is more dominant than adhesive wear. More regions exposed the oxidation, however, a small section of surface harmed by adhesive type wear. On the other hand, parallel lines are placed which resulted from the adhesive wear on the nearly all section of surface 2Mn labelled composite material. Nevertheless, mainly material-removing occurred at the surface of 2Zr labelled composite material which emerged from the abrasive wear as the characteristic of ZrO₂ formation.

4. CONCLUSIONS

In a way that depends on differences in amounts of Mn and Zr particles on the Ti-6Al-4V composite material, the stable MnO and ZrO₂ formation gives rise to better hardness and consequently the more wear resistance was obtained. The microstructure of lath α -phase was formed by 2Mn wt% addition to Ti-6Al-4V impart to the best corrosion resistance where the homogeneous formation on grain boundaries of β -phase mainly affects the corrosion attacks rate negatively. Similarly, the Laves phase occurred by addition of Zr particles as wt%2 amount on the grain boundaries of β -phases hindered the corrosion attacks as it makes a role as a barrier to them.

REFERENCES

1. G. Welsch, B. Rodney, C. E.W., Materials properties handbook: titanium alloys, ASM, 1993.
2. K. G. Budinski, Tribological properties of titanium alloys, *Wear*, 151(2): 203-217, 1991.
3. Y. Liu, L. Chen, H. Tang, C. Liu, B. Liu, B. Huang, Design of powder metallurgy titanium alloys and composites, *Materials Science and Engineering: A*, 418(1): 25-35, 2006.
4. Y. Okazaki, Y. Ito, A. Ito, T. Tateishi, Effect of alloying elements on mechanical properties of titanium alloys for medical implants, *Materials Transactions*, 34(12): 1217-1222, 1993.
5. G. Li, J. Li, X. Tian, X. Cheng, B. He, H. Wang, Microstructure and properties of a novel titanium alloy Ti-6Al-2V-1.5 Mo-0.5 Zr-0.3 Si manufactured by laser additive manufacturing, *Materials Science and Engineering: A*, 684: 233-238, 2017.
6. J. Lu, P. Ge, Y. Zhao, Recent development of effect mechanism of alloying elements in titanium alloy design, *Rare Metal Materials and Engineering*, 43(4): 775-779, 2014.
7. Y. Mao, M. Hagiwari, S. Emura, Creep behavior and tensile properties of Mo-and Fe-added orthorhombic Ti-22Al-11Nb-2Mo-1Fe alloy, *Scripta materialia*, 57(3): 261-264, 2007.
8. B. Fu, H. Wang, C. Zou, Z. Wei, The effects of Nb content on microstructure and fracture behavior of near α titanium alloys, *Materials & Design*, 66: 267-273, 2015.
9. R. Schenk, The corrosion properties of titanium and titanium alloys, *Titanium in medicine*, 145-170, 2001.

10. D. Martins, W. Osorio, M. Souza, R. Caram, A. Garcia, Effects of Zr content on microstructure and corrosion resistance of Ti–30Nb–Zr casting alloys for biomedical applications, *Electrochimica Acta*, 53(6): 2809-2817, 2008.
11. F. Haftlang, A. Hanzaki, H. Abedi, D. Preisler, K. Bartha, The subsurface frictional hardening: a new approach to improve the high-speed wear performance of Ti-29Nb-14Ta-4.5 Zr alloy against Ti-6Al-4V extra-low interstitial., *Wear*, 422: 137-150, 2019.
12. S. Dai, W. Yu, C. Feng, X. Yu, Y. Zhang, Influence of Zr content on microstructure and mechanical properties of implant Ti–35Nb–4Sn–6Mo–xZr alloys, *Transactions of Nonferrous Metals Society of China*, 23(5): 1299-1303, 2013.
13. B. Fu, H. Wang, C. Zou, Z. Wei, The influence of Zr content on microstructure and precipitation of silicide in as-cast near α titanium alloys, *Materials Characterization*, 99: 17-24, 2015.
14. E. Kobayashi, S. Matsumoto, H. Doi, T. Yoneyama, H. Hamanaka, Mechanical properties of the binary titanium-zirconium alloys and their potential for biomedical materials, *Journal of Biomedical Materials Research*, 29(8): 943-950, 1995.
15. C. Xia, Z. Zhang, Z. Feng, B. Pan, X. Zhang, M. Ma, R. Liu, effect of zirconium content on the microstructure and corrosion behavior of Ti-6Al-4V-xZr alloys, *Corrosion Science*, 112: 687-695, 2016.
16. S. Supriadi, T. Immanuel, C. Sutowo, G. Lucky, G. Senopati, B. Suharno, Effect of Mn in new β titanium alloy Ti-6Nb-6Mo on corrosion behavior and mechanical properties, *AIP Conference Proceedings*, 2020. India.
17. S. Yi, Effect of Manganese Addition on the Microstructure and Mechanical Properties of Ti-Nb Biomedical Alloys, *IOP Conf. Series: Earth and Environmental Science*, 252: 2019.
18. S. L. De Assis, S. Wolyneć, I. Costa, Corrosion characterization of titanium alloys by electrochemical techniques, *Electrochimica Acta*, 51(8-9): 1815-1819, 2005.
19. C. Rabadia, Y. Liu, L. Wang, H. Sun, L. Zhang, Laves phase precipitation in Ti-Zr-Fe-Cr alloys with high strength and large plasticity, *Materials & Design*, 154: 228-238, 2018.
20. İ. H. Kara, H. Ahlatcı, Y. Türen, Y. Sun, Microstructure and corrosion properties of lanthanum-added AZ31 Mg alloys, *Arabian Journal of Geosciences*, 11: 535, 2018.
21. M.E. Turan, Y. Sun, F. Aydın, Y. Akgul, Influence of multi-wall carbon nanotube content on dry and corrosive wear performances of pure magnesium, *Journal of Composite Materials*, 0(0), 1–9, 2018.